Review of Lecture 8

- Blackbody function
- Earth motion
- Solar spectra: AM0, AM1, AM1.5 etc.
- Definition of radiative properties
- Maximum efficiency of solar thermal engines
- Maximum achievable temperature
- Wavelength (frequency) selective surfaces

Contents of lecture 9

- Solar hot water systems
- Maximum solar concentration
- Methods for concentration
- Nontracking and tracking
- Solar thermal-mechanical energy conversion
- EM wave calculation of surface properties

Solar Hot Water Systems

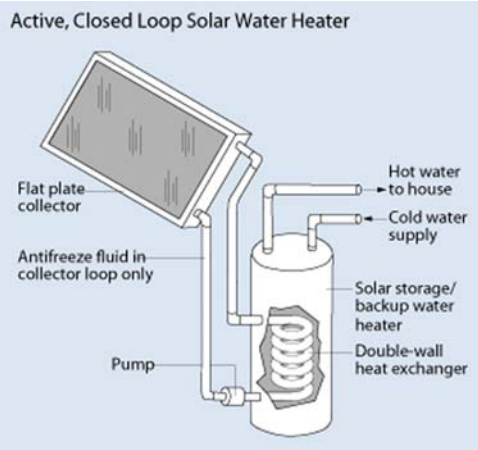

http://78.136.49.147/images/Solar%20Hot%20Water%20Heating%20Diagram.gif

Image by EERE.

How Much Area You Need?

- **80 Gallon of Water**
- **Start temperature T_i=15 ºC**
- **Hot water temperature T_f=60 ºC**

Energy Balance

$$A \bullet J_s \bullet \Delta t \bullet \eta = mc\left(T_f - T_i\right)$$

$$\Delta t = 5.5 \text{ hours/day}$$

Specific heat c= 4180 J/kg.K

J_s=1000 W/m^2

Thermal efficiency η=60%

A=5.1 m^2

Flat Panel Solar Hot Water Heaters

Images removed due to copyright restrictions.
Please also see:
http://greennav.files.wordpress.com/2008/03/solar-panel.gif

http://www.mdelectric.ca/1_Pictures/Green Energies/GE-ViessmannCollector.jpg

http://collector-solar.com/products/index.htm

Photo by szczel on Flickr.

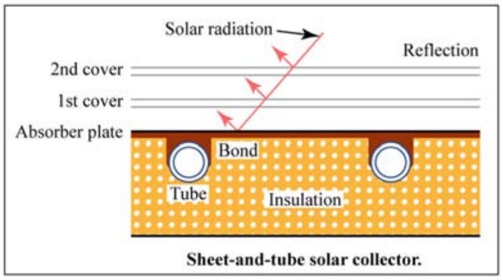

Sheet-and-tube solar collector.

Figure by MIT OpenCourseWare.

Evacuated Tube Technology

Images removed due to copyright restrictions. Please see:

http://img.diytrade.com/cdimg/194777/1624552/0/1160536024/All-Glass_Evacuated_Solar_Collector_Tube-SFVA.jpg

http://img.diytrade.com/cdimg/194777/1624568/0/1160536058/All-Glass_Evacuated_Solar_Collector_Tube-SFVB.jpg

http://img.diytrade.com/cdimg/194777/1624573/0/1160536136/Metal-Glass_Evacuated_Solar_Collector_Tube-SFVC.jpg

http://www.diytrade.com/china/4/products/1716424/All-Glass_Evacuated_Solar_Collector_Tube-SFVA.html

Vacuum Tube Hot Water Heaters

Images removed due to copyright restrictions. Please see any photos of solar water heaters, such as:

http://image.made-in-china.com/2f0j00ferESMmCAVoH/Solar-Collector.jpg

http://image.made-in-china.com/2f0j00VBdtYnQhIaRE/Split-Pressurized-Solar-Water-Heater-CY-SP-24-.jpg

Unpressurized

Separate Tank Collector

Efficiency Estimation---Evacuated Tubes

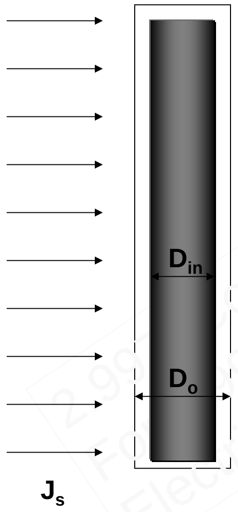

Incoming Solar Radiation

$$Q_{in} = D_o \bullet L \bullet J_s$$

Absorbed Solar Radiation

$$Q_a = D_i \bullet L \bullet J_s \bullet \tau \bullet \alpha$$

Radiation Loss

$$Q_{loss} = \varepsilon(\pi D_i L)\sigma\left[T_s^4 - T_a^4\right]$$

Thermal Efficiency

$$\eta = \frac{Q_a - Q_{loss}}{Q_{in}} = \frac{D_i}{D_o}\left(\alpha\tau - \frac{\pi\varepsilon\sigma}{J_s}\left[T_s^4 - T_a^4\right]\right)$$

Efficiency Estimation---Flat Panel

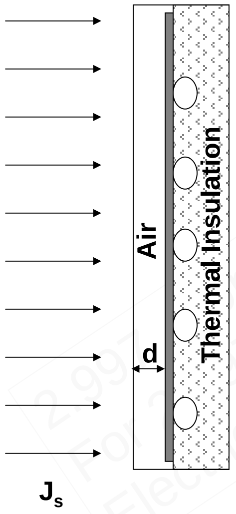

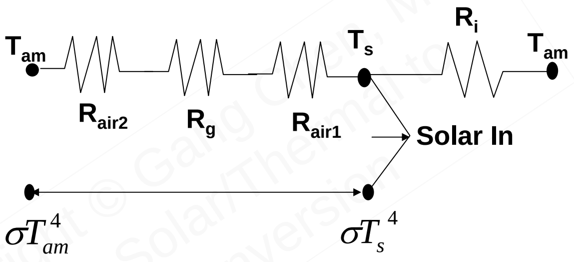

$$R_{air1} = \frac{d}{k_{air}A} \approx \frac{10\times10^{-3}}{0.026A} = \frac{0.38}{A}\,[\mathrm{K/W}]$$

$$R_g = \frac{d_g}{k_g A} \approx \frac{0.3\times10^{-3}}{1.2A} = \frac{0.00025}{A}\,[\mathrm{K/W}]$$

$$R_{air2} = \frac{1}{hA} \approx \frac{1}{5A} = \frac{0.2}{A}\,[\mathrm{K/W}]$$

$$R_i = \frac{d_i}{k_i A} \approx \frac{3\times10^{-2}}{0.1A} = \frac{0.3}{A}\,[\mathrm{K/W}]$$

Efficiency Estimation---Flat Panel

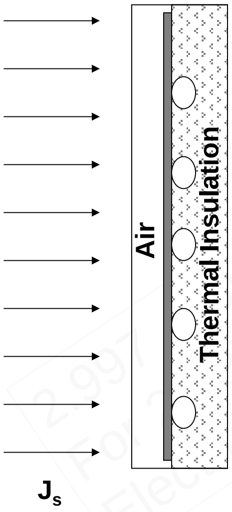

$$Q_{loss} = \frac{T_s - T_{am}}{R_{air1} + R_{air2} + R_g} + \frac{T_s - T_{am}}{R_i} + \varepsilon\sigma A\left[T_s^4 - T_{am}^4\right]$$

$$= 5.5A\left[T_s - T_{am}\right] + \varepsilon\sigma A\left[T_s^4 - T_{am}^4\right]$$

Thermal Efficiency

$$\eta = \frac{Q_a - Q_{loss}}{Q_{in}}$$

$$= \alpha\tau - \frac{1.7\left[T_s - T_{am}\right]}{J_s} - \frac{\pi\varepsilon\sigma}{J_s}\left[T_s^4 - T_a^4\right]$$

Estimated and Experimental Results

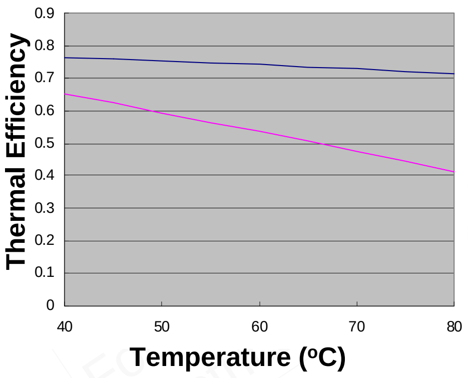

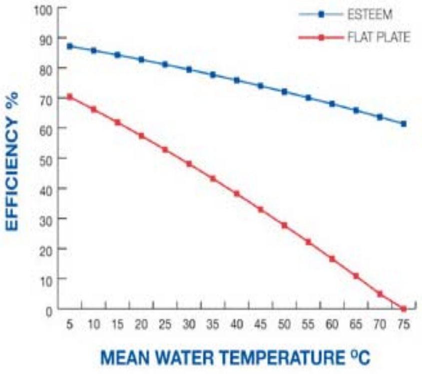

http://www.enviro-friendly.com/images/NSW-Winter-Solar-Efficiency-graph.jpg

Courtesy of Hills Solar. Used with permission.

Total Renewable Capacity in 2007

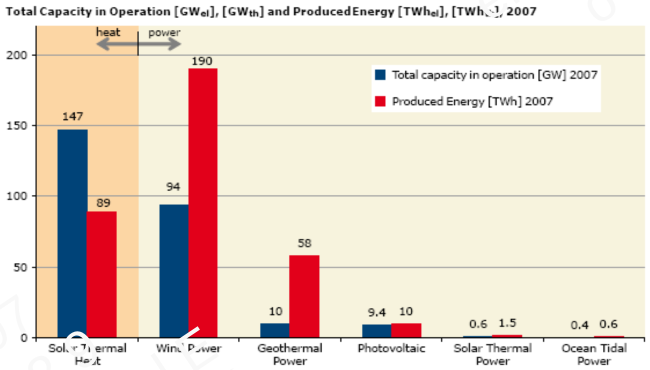

Courtesy of IEA-SHC. Used with permission.

Weiss et al., Solar Heat Worldwide, 2009 Ed.

Solar Heat Utilization

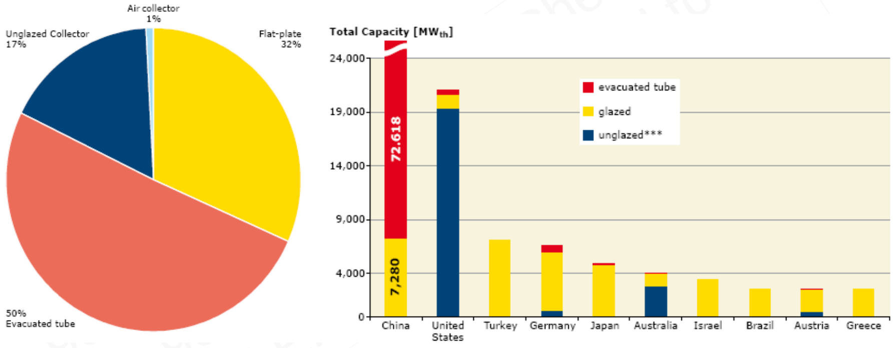

Courtesy of IEA-SHC. Used with permission.

Weiss et al., Solar Heat Worldwide, 2009 Ed.

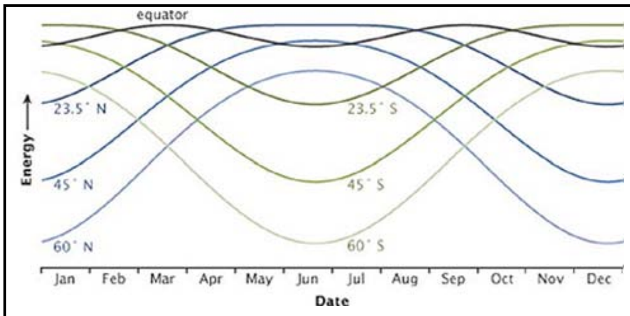

Earth Orbital

Image by Robert Simmon (NASA).

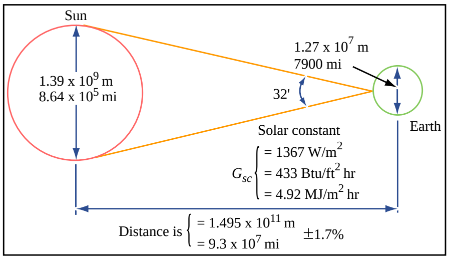

Figure by MIT OpenCourseWare.

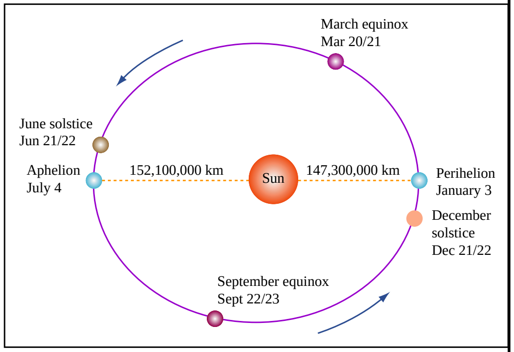

Figure by MIT OpenCourseWare.

Maximum Concentration of Sun Light---2nd Law Limit

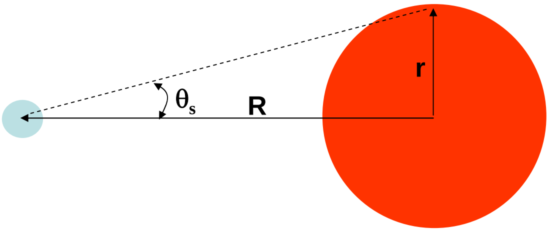

Energy Balance

$$4\pi r^2 J_s = 4\pi R^2 J_e$$

With Concentration

$$CJ_e = \sigma T_c^{\,4} \le \sigma T_s^{\,4} = J_s$$

Maximum concentration

$$C_{\max} = \frac{J_s}{J_e} = \left(\frac{R}{r}\right)^2$$

$$= \frac{1}{\sin^2 \theta_s} = 46{,}164$$

Maximum Concentration of Sun Light---2nd Law Limit

Inside a medium of refractive index n

$$CJ_e = n\sigma T_c^{\,4}$$

$$C_{\max} = \frac{n^2}{\sin^2\theta}$$

Image removed due to copyright restrictions
Please see Fig. 1a in Gleckman, Philip, Joseph O'Gallagher, and Roland Winston. "Concentration of Sunlight to Solar-surface Levels Using Non-imaging Optics." *Nature* 339 (1989): 198-200.

Achieved C=56,000

Gleckman et al., Nature, 339, 198 (1989)

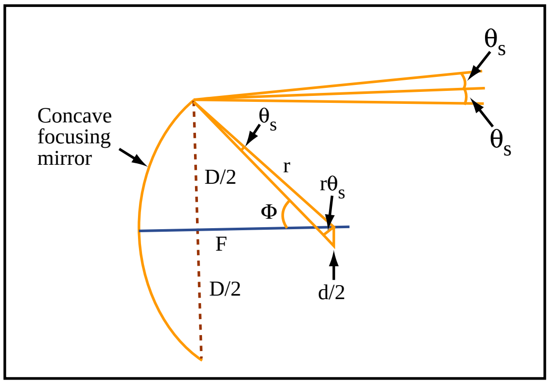

Figure by MIT OpenCourseWare.

2D Flat Panel

$$r\sin\theta_s = \frac{d}{2}\cos\Phi$$

$$r\sin\Phi = \frac{D}{2}$$

$$\frac{D}{d} = \frac{\sin\Phi\cos\Phi}{\sin\theta_s} = \frac{\sin 2\Phi}{2\sin\theta_s}$$

$$C_{\max} = \frac{1}{2\sin\theta_s} = 107$$

3D Concentration $C_{\max} = \dfrac{1}{4\sin^2\theta_s}$

Imaging Concentration to Cylinder

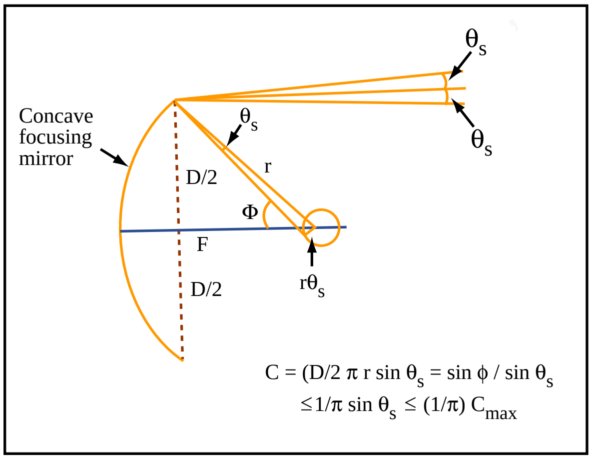

$C = (D/2\ \pi\ r \sin\theta_s = \sin\phi / \sin\theta_s$

$\leq 1/\pi \sin\theta_s \leq (1/\pi)\ C_{max}$

Figure by MIT OpenCourseWare.

From Fig.4.3: R. Winston et al., Nonimaging Optics, Elsevier, 2005

Nonimaging Optics

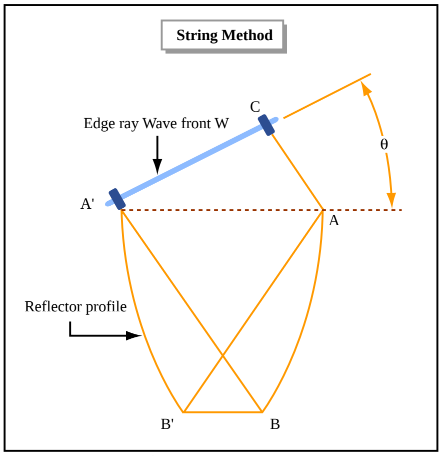

Figure by MIT OpenCourseWare.

2D Concentration to Flat Plate

$$AC + AB' = A'B + BB'$$

$$AB' = A'B$$

$$AC = AA'\sin\theta$$

$$C = \frac{AA'}{BB'} = \frac{1}{\sin\theta}$$

3D Concentration $C = \left(\frac{1}{\sin\theta}\right)^2$

Maximum when $\theta = \theta_s$

2D Concentration to Cylinder

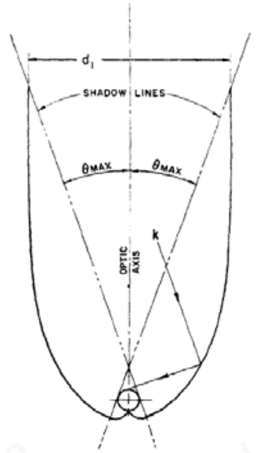

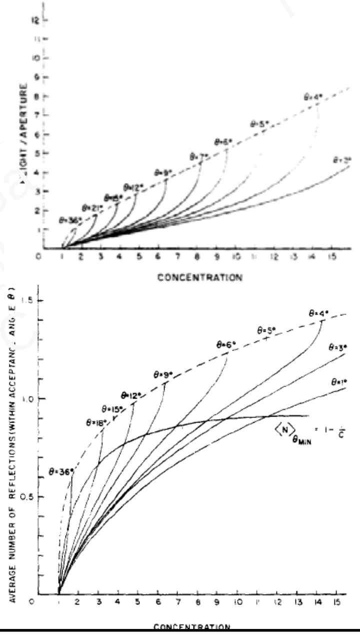

Winston and Hinterberger, Solar Energy, 17, 255 (1975)

Courtesy of Elsevier, Inc., http://www.sciencedirect.com. Used with permission.

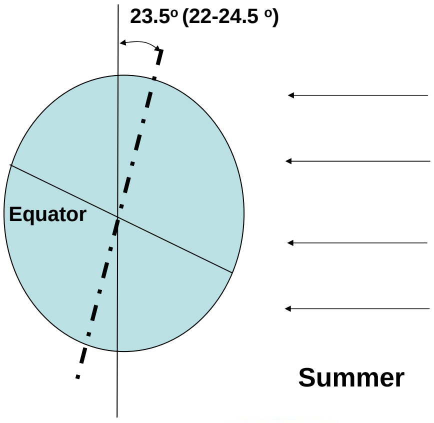

Summer

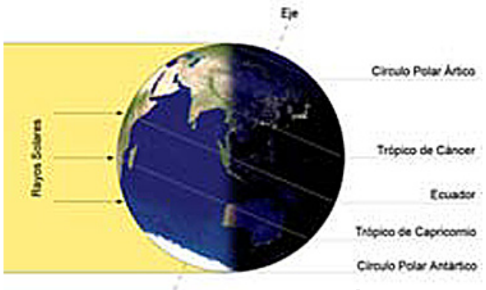

Winter

Images from Wikimedia Commons, http://commons.wikimedia.org

Earth Orbital

Daily Insolation Variation

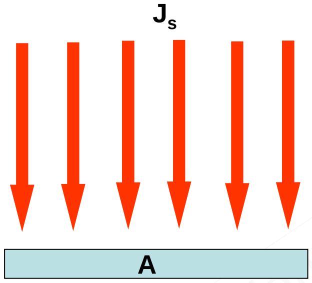

At Noon: $Q=J_sA$

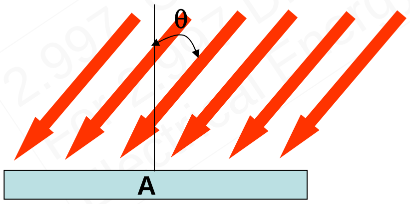

$Q= J_sA\sin\theta$

J_s also varies due to path length

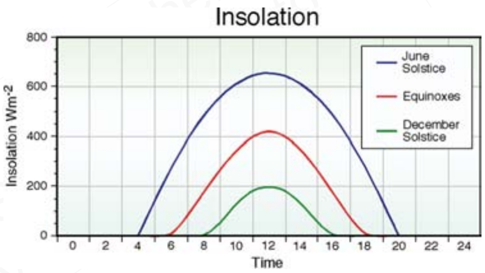

45º North Latitude
http://www.eoearth.org/article/Daily_and_annual_cycles_of_temperature

Courtesy of Michael Pidwirny. Used with permission.

Tracking

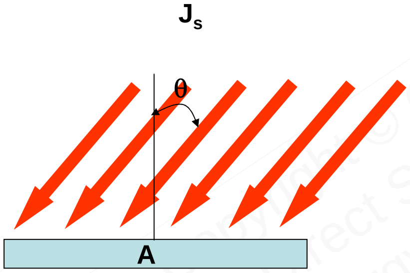

$Q= J_sA\sin\theta$

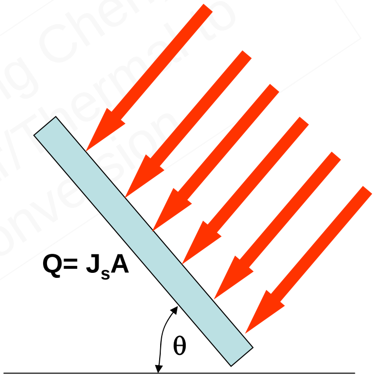

One Axis: Axis Along South-North Direction

V-Trough

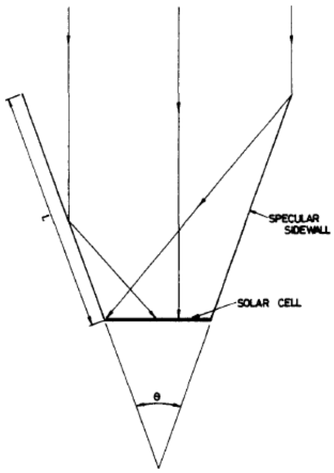

- **East-West Orientation, with seasonal adjustment: 2.5-3 times**
- **South-North tracking**

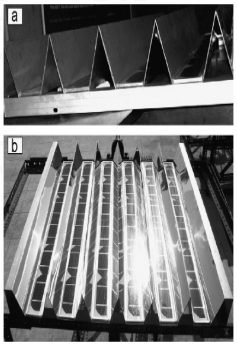

Holland, Solar Energy, 13, 149 (1971)

http://www.electricksolutions.com/cms/templates/electriksolutions/IMAGES/banner1.jpg

Courtesy of Elsevier, Inc., http://www.sciencedirect.com.
Used with permission.

Solar Thermal Energy Conversion ---Mechanical Systems

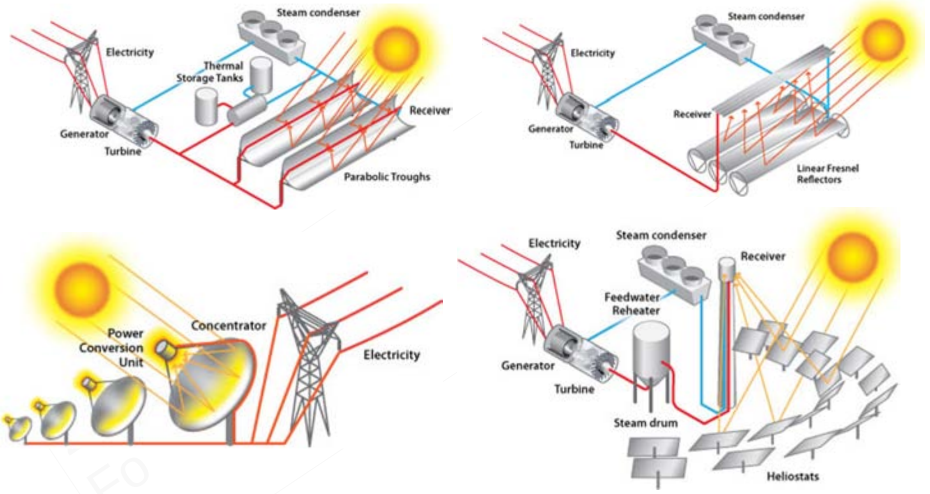

Images by EERE. Please also see Fig. 21-13 in Kreith, Frank, and D. Yogi Goswami. *Handbook of Energy Efficiency and Renewable Energy*. Boca Raton, FL: CRC Press, 2007.

Handbook of Energy Efficiency and Renewable Energy

Solar Trough

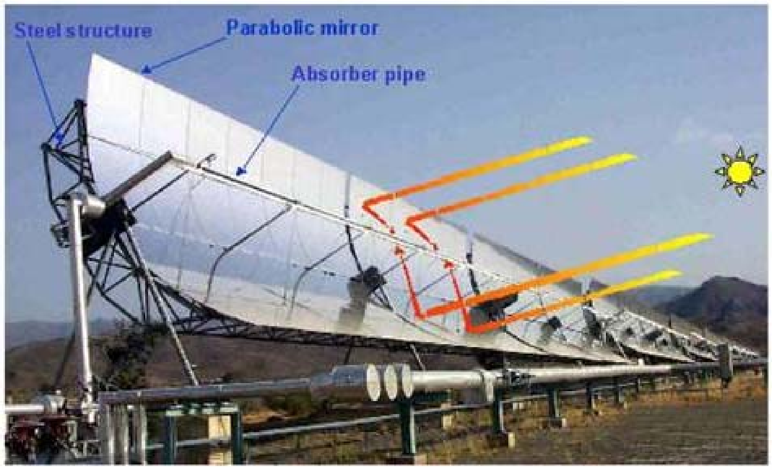

Courtesy of Plataforma Solar de Almería. Used with permission.

Solar Trough

Image removed due to copyright restrictions.
Please see Fig. 5.16 in Kaltschmitt, Martin, Wolfgang Streicher, and Andreas Weise.
Renewable Energy: Technology, Economics, and Environment. New York, NY: Springer, 2007.
Also see any photo of a commercial HCE, such as Schott's PTR 70.

Solar Trough with Molten Salt Storage

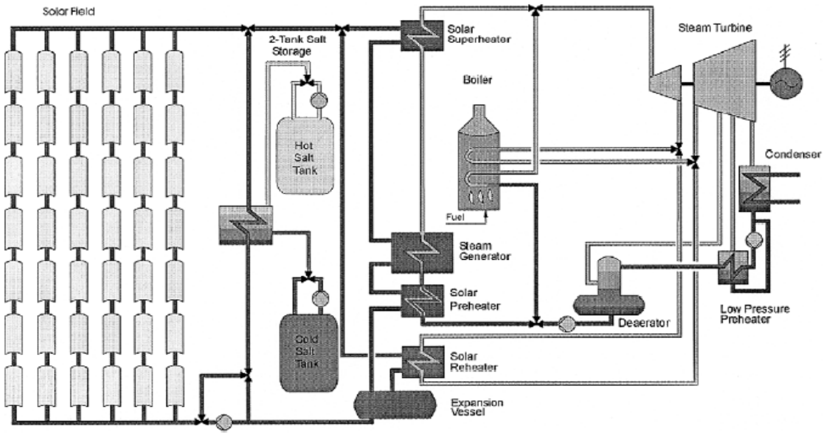

Courtesy of Elsevier, Inc., http://www.sciencedirect.com. Used with permission.

Price, H. Lupfert, E.“Advances in Parabolic Trough Solar Power Technology”

Line Concentration Systems

- *Most mature concentrated solar thermal technology*
- *380 MWe installed*
- *About 1000 MWe of new contracts issued*
- *Favorable unit size range 50-100MWe*

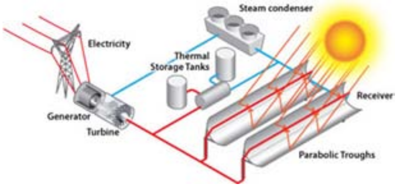

Photos by EERE, Sandia National Labs.

Commercial Trough System in California

Image removed due to copyright restrictions. Please see any photo of a linear Fresnel lens system, such as http://commons.wikimedia.org/wiki/File:Fresnel_reflectors_ausra.jpg http://i.i.com.com/cnwk.1d/i/ne/p/2007/910Ausra1_550x367.jpg

From J. Karni

Courtesy of Jacob Karni. Used with permission.

Solar Trough: Concentration Ratio

Table removed due to copyright restrictions.
Please see Table 2 in Price, Hank, et al.
"Advances in Parabolic Trough Solar Power Technology."
Journal of Solar Energy Engineering 124 (May 2002): 109-125.

Price, H. Lupfert, E.“Advances in Parabolic Trough Solar Power Technology”

Solar Trough: Cost

Table removed due to copyright restrictions.
Please see Table 8 in Price, Hank, et al.
"Advances in Parabolic Trough Solar Power Technology."
Journal of Solar Energy Engineering 124 (May 2002): 109-125.

Price, H. Lupfert, E.“Advances in Parabolic Trough Solar Power Technology”

Trough Efficiency

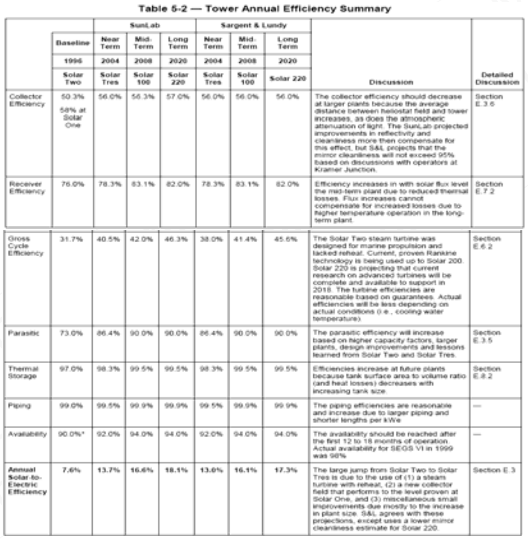

Table 5-2 — Tower Annual Efficiency Summary

		SunLab			Sargent & Lundy				
	Baseline	Near Term	Mid-Term	Long Term	Near Term	Mid-Term	Long Term		
	1996	2004	2008	2020	2004	2008	2020		
	Solar Two	Solar Tres	Solar 100	Solar 220	Solar Tres	Solar 100	Solar 220	Discussion	Detailed Discussion
Collector Efficiency	50.3% 58% at Solar One	56.0%	56.3%	57.0%	56.0%	56.0%	56.0%	The collector efficiency should decrease at larger plants because the average distance between heliostat field and tower increases, as does the atmospheric attenuation of light. The SunLab projected improvements in reflectivity and cleanliness more then compensate for this effect, but S&L projects that the mirror cleanliness will not exceed 95% based on discussions with operators at Kramer Junction.	Section E.3.6
Receiver Efficiency	76.0%	78.3%	83.1%	82.0%	78.3%	83.1%	82.0%	Efficiency increases in with solar flux level the mid-term plant due to reduced thermal losses. Flux increases cannot compensate for increased losses due to higher temperature operation in the long-term plant.	Section E.7.2
Gross Cycle Efficiency	31.7%	40.5%	42.0%	46.3%	38.0%	41.4%	45.6%	The Solar Two steam turbine was designed for marine propulsion and lacked reheat. Current, proven Rankine technology is being used up to Solar 200. Solar 220 is projecting that current research on advanced turbines will be complete and available to support in 2018. The turbine efficiencies are reasonable based on guarantees. Actual efficiencies will be less depending on actual conditions (i.e., cooling water temperature).	Section E.6.2
Parasitic	73.0%	86.4%	90.0%	90.0%	86.4%	90.0%	90.0%	The parasitic efficiency will increase based on higher capacity factors, larger plants, design improvements and lessons learned from Solar Two and Solar Tres.	Section E.3.5
Thermal Storage	97.0%	98.3%	99.5%	99.5%	98.3%	99.5%	99.5%	Efficiencies increase at future plants because tank surface area to volume ratio (and heat losses) decreases with increasing tank size.	Section E.8.2
Piping	99.0%	99.5%	99.9%	99.9%	99.5%	99.9%	99.9%	The piping efficiencies are reasonable and increase due to larger piping and shorter lengths per kWe	—
Availability	90.0%*	92.0%	94.0%	94.0%	92.0%	94.0%	94.0%	The availability should be reached after the first 12 to 18 months of operation. Actual availability for SEGS VI in 1999 was 98%	—
Annual Solar-to-Electric Efficiency	**7.6%**	**13.7%**	**16.6%**	**18.1%**	**13.0%**	**16.1%**	**17.3%**	The large jump from Solar Two to Solar Tres is due to the use of (1) a steam turbine with reheat, (2) a new collector field that performs to the level proven at Solar One, and (3) miscellaneous small improvements due mostly to the increase in plant size. S&L agrees with these projections, except uses a lower mirror cleanliness estimate for Solar 220.	Section E.3

"Assessment of Parabolic Trough and Power Tower Solar Technology Cost and Performance Forecasts" NREL, 2003

Trough Cost Breakdown

Figure 4-1 — Major Cost Categories for Parabolic Trough Plant
2004 Near-Term Case: 100 MWe, 12 hours TES, 2.5 Solar Multiple

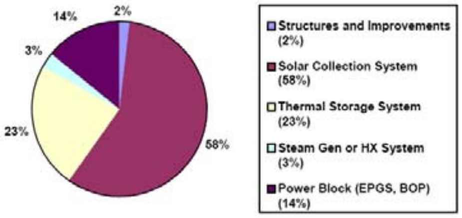

Figure 4-2 — Solar Field Component Cost Breakdown for Parabolic Trough Plant
2004 Near-Term Case: 100 MWe, 12 hours TES, 2.5 Solar Multiple

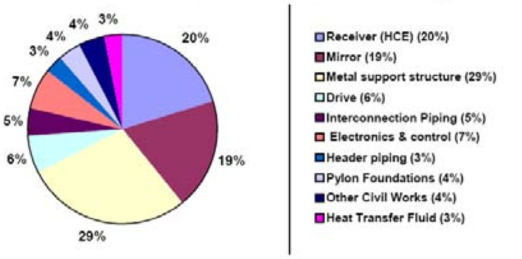

"Assessment of Parabolic Trough and Power Tower Solar Technology Cost and Performance Forecasts" NREL, 2003

Heliostat / Power Tower

Photo by Koza1983 on Wikipedia.

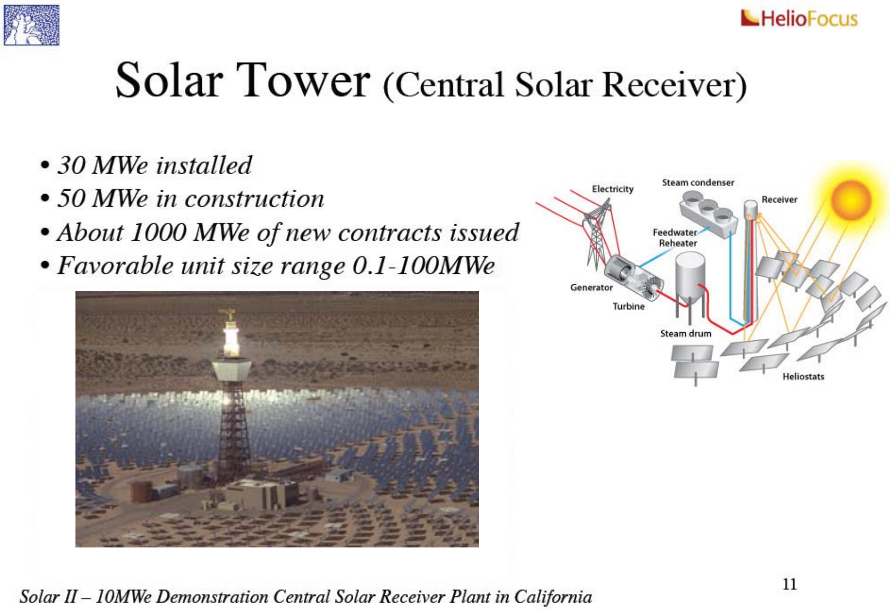

Solar Tower (Central Solar Receiver)

- *30 MWe installed*
- *50 MWe in construction*
- *About 1000 MWe of new contracts issued*
- *Favorable unit size range 0.1-100MWe*

Solar II – 10MWe Demonstration Central Solar Receiver Plant in California

Images by EERE and Sandia National Laboratory.

Courtesy of Jacob Karni. Used with permission.

From J. Karni

Heliostat Receiver

Images removed due to copyright restrictions.
Please see Fig. 21-49. 21-51, and Table 21-9 in Kreith, Frank, and D.
Yogi Goswami. *Handbook of Energy Efficiency and Renewable Energy*.
Boca Raton, FL: CRC Press, 2007.

Handbook of Energy Efficiency and Renewable Energy

Heliostat / Power Tower Cost

Image removed due to copyright restrictions.
Please see Fig. 21-40 in Kreith, Frank, and D. Yogi Goswami.
Handbook of Energy Efficiency and Renewable Energy.
Boca Raton, FL: CRC Press, 2007.

Handbook of Energy Efficiency and Renewable Energy

Heliostat / Power Tower Efficiency

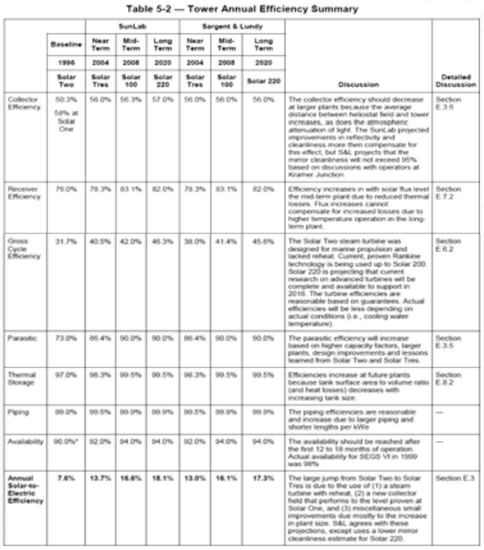

Table 5-2 — Tower Annual Efficiency Summary

		SunLab			Sargent & Lundy				
	Baseline	**Near Term**	**Mid-Term**	**Long Term**	**Near Term**	**Mid-Term**	**Long Term**		
	1996	**2004**	**2008**	**2020**	**2004**	**2008**	**2020**		
	Solar Two	**Solar Tres**	**Solar 100**	**Solar 220**	**Solar Tres**	**Solar 100**	**Solar 220**	**Discussion**	**Detailed Discussion**
Collector Efficiency	50.3% 58% at Solar One	56.0%	56.3%	57.0%	56.0%	56.0%	56.0%	The collector efficiency should decrease at larger plants because the average distance between heliostat field and tower increases, as does the atmospheric attenuation of light. The SunLab projected improvements in reflectivity and cleanliness more then compensate for this effect, but S&L projects that the mirror cleanliness will not exceed 95% based on discussions with operators at Kramer Junction.	Section E.3.6
Receiver Efficiency	76.0%	78.3%	83.1%	82.0%	78.3%	83.1%	82.0%	Efficiency increases in with solar flux level the mid-term plant due to reduced thermal losses. Flux increases cannot compensate for increased losses due to higher temperature operation in the long-term plant.	Section E.7.2
Gross Cycle Efficiency	31.7%	40.5%	42.0%	46.3%	38.0%	41.4%	45.6%	The Solar Two steam turbine was designed for marine propulsion and lacked reheat. Current, proven Rankine technology is being used up to Solar 200. Solar 220 is projecting that current research on advanced turbines will be complete and available to support in 2018. The turbine efficiencies are reasonable based on guarantees. Actual efficiencies will be less depending on actual conditions (i.e., cooling water temperature).	Section E.6.2
Parasitic	73.0%	86.4%	90.0%	90.0%	86.4%	90.0%	90.0%	The parasitic efficiency will increase based on higher capacity factors, larger plants, design improvements and lessons learned from Solar Two and Solar Tres.	Section E.3.5
Thermal Storage	97.0%	98.3%	99.5%	99.5%	98.3%	99.5%	99.5%	Efficiencies increase at future plants because tank surface area to volume ratio (and heat losses) decreases with increasing tank size.	Section E.8.2
Piping	99.0%	99.5%	99.9%	99.9%	99.5%	99.9%	99.9%	The piping efficiencies are reasonable and increase due to larger piping and shorter lengths per kWe	—
Availability	90.0%*	92.0%	94.0%	94.0%	92.0%	94.0%	94.0%	The availability should be reached after the first 12 to 18 months of operation. Actual availability for SEGS VI in 1999 was 98%	—
Annual Solar-to-Electric Efficiency	**7.6%**	**13.7%**	**16.6%**	**18.1%**	**13.0%**	**16.1%**	**17.3%**	The large jump from Solar Two to Solar Tres is due to the use of (1) a steam turbine with reheat, (2) a new collector field that performs to the level proven at Solar One, and (3) miscellaneous small improvements due mostly to the increase in plant size. S&L agrees with these projections, except uses a lower mirror cleanliness estimate for Solar 220.	Section E.3

“Assessment of Parabolic Trough and Power Tower Solar Technology Cost and Performance Forecasts” NREL, 2003

Dish

Photo from Wikimedia Commons, http://commons.wikimedia.org

Dish and Stirling Engine

Images removed due to copyright restrictions.
Please see Fig. 5.20, 5.21, and 5.22 in Kaltschmitt, Martin, Wolfgang Streicher, and Andreas Weise. *Renewable Energy: Technology, Economics, and Environment*. New York, NY: Springer, 2007.

Kaltschmitt, M.,Wolfgang, S. Wiese, A. “Renewable Energy, technology, Economics and Enviroment”

Dish and Stirling Engine

Table removed due to copyright restrictions.
Please see Table 5.10 in Kaltschmitt, Martin, Wolfgang Streicher, and Andreas Weise. *Renewable Energy: Technology, Economics, and Environment*. New York, NY: Springer, 2007.

Kaltschmitt, M.,Wolfgang, S. Wiese, A. “Renewable Energy, technology, Economics and Enviroment”

EM Waves

Maxwell Equations:

$$\nabla \times \mathbf{E} = -\frac{\partial \mathbf{B}}{\partial t}$$

$$\nabla \times \mathbf{H} = \frac{\partial \mathbf{D}}{\partial t} + \mathbf{J}_{\mathbf{e}}$$

$$\nabla \bullet \mathbf{D} = \rho_e$$

$$\nabla \bullet \mathbf{B} = 0$$

E --- Electric Field
H --- Magnetic Field
D --- Electric Displacement
B --- Magnetic Induction
$\mathbf{J}_e$ --- Free Current Density

- **Constitutive Relations**

$\mathbf{D} = \varepsilon \mathbf{E}$

$\mathbf{B} = \mu \mathbf{H}$

ε – Electric Permitivity
μ – Magnetic permeability

EM Wave Propagation inside A Medium

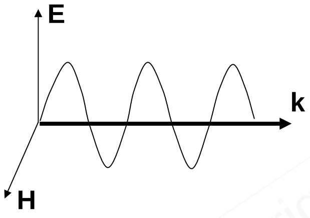

ω**--- angular frequency**
k --- Wavevector

$\hat{\mathbf{k}}$ --- Unit Wavevector

N=n+iκ,
Complex refractive index
κ --- Extinction coefficient

- **Plane Wave Solution**

$$\mathbf{E}(\mathbf{r},t) = \mathbf{E}_o \exp\left[-i\omega\left(t - \frac{N}{c_o}\hat{\mathbf{k}} \bullet \mathbf{r}\right)\right]$$

$$\mathbf{H}(\mathbf{r},t) = \mathbf{H}_o \exp\left[-i\omega\left(t - \frac{N}{c_o}\hat{\mathbf{k}} \bullet \mathbf{r}\right)\right]$$

- **Poynting Vector (Energy Flux)**

$$\mathbf{S}(\mathbf{r}) = \frac{1}{2}\mathrm{Re}\left[\mathbf{E} \times \mathbf{H}^*\right]$$

$$\mathbf{S} = \frac{1}{2}\frac{n}{\mu c_o} e^{-\alpha x}\left|\mathbf{E}\right|^2 \hat{\mathbf{k}}$$

$$\alpha = \frac{4\pi\kappa}{\lambda_o}$$

Absorption Coefficient

EM Wave Reflection and Transmission at An Interface

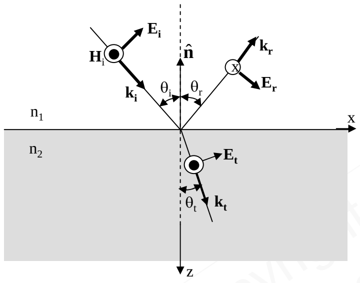

Symbol Convention:

- ◉ **Field Going Out of Paper**
- ⊗ **Field Going Into Paper**

E-Field In the Plane of Incidence:

TM Wave = // Wave = p Wave

H-Field In the Plane of Incidence:

TE Wave = ⊥Wave = s Wave

- **Snell Law**

$$\theta_i=\theta_r$$

$$n_1 \sin\theta_i = n_2 \sin\theta_t$$

- **Fresnel Coefficients**

$$r_{//} = \frac{E_{//r}}{E_{//i}} = \frac{-n_2\cos\theta_i + n_1\cos\theta_t}{n_2\cos\theta_i + n_1\cos\theta_t}$$

$$t_{//} = \frac{E_{//t}}{E_{//i}} = \frac{2n_1\cos\theta_i}{n_2\cos\theta_i + n_1\cos\theta_t}$$

- **Reflectivity/transmissivity**

$$R_{//} = \left|r_{//}\right|^2 \qquad \tau_{//} = \frac{\mathrm{Re}(N_2\cos\theta_t)}{\mathrm{Re}(N_1\cos\theta_i)}\left|t_{//}\right|^2$$

Examples

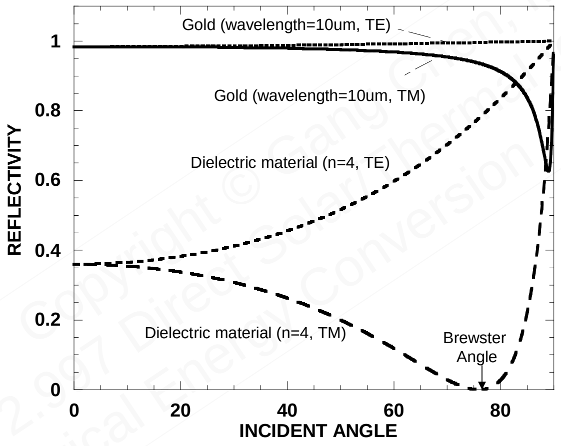

Reflectivity as a function of the angle of incidence for a dielectric material with n=4 and for gold with N=10.8+i51.6.

2.997 Direct Solar/Thermal to Electrical Energy Conversion Technologies
Fall 2009